Impact of Lossy Compression on the Classification of Remotely-Sensed Imagery Data

John A. Saghri
Electrical Engineering Dept., Cal Poly, San Luis Obispo, California

Andrew G. Tescher▲
Compression Science Inc., Campbell, California

The impact of lossy compression on classification of remotely–sensed imagery data is examined. The impact of compression is assessed for two types of classifications: unsupervised classification via thematic map for small-footprint imagery, and supervised classification via spectral unmixing for large-footprint imagery data. An overview of viable classification and spectral unmixing procedures are given. The criteria for measuring the impact of compression are defined. Simulation results using NOAA's AVHRR (1.1 km footprint), and LANDSAT 5 TM (30 m footprint) test imagery, show that the impact of compression is insignificant for compression ratios of less than 8. It is argued that the effective impact of compression is reduced due to the presence of other sources of inaccuracy in the original data and its relevant prediction models.

Journal of Imaging Science and Technology 46: 575–582 (2002)

Introduction

Images acquired by sensors on board earth observation satellites and scientific probes represent large volumes of data. This data need to be stored on board and/or transmitted to ground stations for processing. As sensor technology evolves into the 21st century, the volume of data will increase rapidly due to utilization of sensors that, in addition to having high spatial and dynamic resolutions, have high spectral resolution covering up to several hundred bands. This large volume of data creates challenging problems for both onboard storage (due to the stringent limitations on power, weight, and size) and transmission to ground stations (due to bandwidth limitation on downlink channels). It is therefore imperative to reduce the volume of data to a minimum via bandwidth compression techniques. Lossless compression of data is ideal but the amount of compression achievable is bound by the entropy of the source. This entropy bound limits the obtainable amount of compression to the range of two to three. This level of compression is inadequate to alleviate the onboard storage and downlink transmission problems. For this reason there have numerous efforts by researchers to develop near lossless compression algorithms. Lossy compression entails a certain amount of loss in the fidelity of data based on the level of compression. The image quality must be compatible with all the potential uses to which images may be put. Therefore the chosen algorithm must be very robust with respect to image processing usually applied (normalization, deconvolution, filtering, resampling, etc.)[1]

In general the quality of the final product obtained from the data depends on the precision of the original data as well as the accuracy of the relevant exploitation algorithm. Lossy compression of the sensor data becomes an additional factor in the quality of the final product. For certain meteorological applications including sea surface temperature and cloud mask determination, it has been shown that the additional distortion at low to moderate compression ratio, is quantifiable and within the range of other distortions.[2]

In this article we examine the impact of lossy of compression on the classification of the remotely–sensed imagery data. The impact of compression is assessed for two types of classifications; unsupervised classification via thematic map for small-footprint imagery, and supervised classification via spectral unmixing for large-footprint imagery data. Classification is the most widely used method for extracting information on surface cover. Conventional classification techniques assign a single label to each pixel. The label can be any one of the known categories such as water, forest, soil, and rock. The resulting thematic map can become a very useful land cover interpretive aid provided that the imagery data is composed of pure pixels, meaning that each pixel represents the spectral signature of only one species. A thematic map is thus appropriate for imagery data with a relatively small footprint, i.e., ground sampling distance

Original manuscript received September 24, 2001

▲ IS&T Member

*Corresponding authors email: jsaghri@calpoly.edu; andytescher@attbi.com

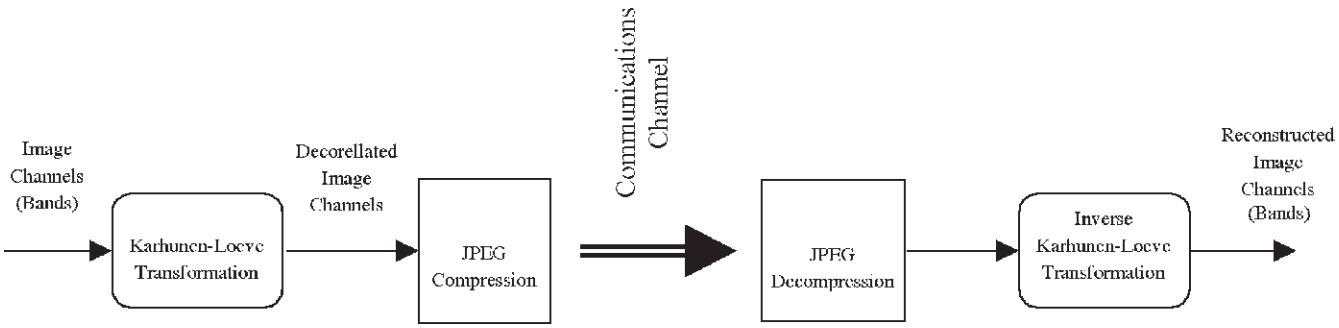

Figure 1. Adopted KLT/JPEG compression approach

(GSD) such as LANDSAT Thematic Mapper imagery with a 30 m footprint. For large-foorprint imagery, such as those from NOAA's AVHRR sensor with a 1.1 km footprint, accurate land cover estimation can only be achieved if each pixel is assigned not just to one, but several labels along with their respective concentrations in that pixel's footprint. The technique used to assign these labels and proportions is known as mixture modeling, or spectral unmixing. Spectral unmixing produces a compositional map, also known as abundance image, that provides a more complete land cover type information than a thematic map. The set of compositional maps depicts the proportions of all species present in each pixel footprint, while the thematic map identifies only the species with the highest concentration. Thus it can be argued that spectral unmixing yields more complete classification information than a thematic map. Since the number and the signatures of species in the scene is provided in advance, the process of spectral unmixing can be considered as a "supervised" form of classification for large-footprint imagery.

The selected compression technique was the adaptive Karhhnen–Loeve transform/JPEG (KLT/JPEG) method previously developed.[3,4] Images are first spectrally decorrelated via KLT and then individually coded via standard JPEG as shown in Fig. 1. The impact of compression is examined for both types of classifications, i.e., classification via thematic map for small-footprint imagery, and classification via spectral unmixing (decomposition into abundance images) for large-footprint imagery data. A description of classification and spectral unmixing procedures and the definition of the criteria for measuring the impact of compression are given in the following sections.

Classification of Small-Footprint Spectral Imagery Data

Classification of the pixels representing a remotely sensed image, is the process of associating each pixel with a label describing an entity, e.g., soil, water, or vegetation, on the ground. So classification can be regarded as the problem of recognition of the remotely sensed area according to the gray scale values associated with each pixel vector. These values identify the observable geographical, geological or other Earth surface characteristics. We can expect an automatic classification procedure to label pixel vectors on the basis of comparison with the spectral reflectance characteristics (spectral signature) of objects (entities) well known. If this labeling operation is carried out for all pixels in the area then the result is a *thematic map* which shows the geographical distribution of a theme such as water rather than the multifarious details in each place as represented on a topographical map. The classified remotely sensed image is thus a form of digital thematic map and, if the geometry is transformed so as to match a recognized map projection, it is in a form suitable for incorporation into a digital geographic information system (GIS).

The problem of allocating individual pixels to their most likely class, i.e., labeling the pixels, can be approached in one of two ways; supervised and unsupervised classifications. If we know the number of separable patterns that exist in the geographical area covered by the image, and if we can estimate the statistical characteristics of the values taken on by the features describing each of these patterns, then a series of templates can be built up. This is referred to as supervised classification. Each template represents an ideal pattern. The individual pixels can be compared with each template in turn and the closest match found. Each pixel is therefore labeled as belonging to the class represented by the most similar template. In the alternative unsupervised classification, no knowledge of the number or character of the patterns present in the image is assumed initially. Instead, a method of allocating and reallocating the individual pixels to one of an initial set or arbitrarily chosen patterns is used. These will be called "basic patterns". At each stage each pixel in turn is given the label of one of these basic patterns using some decision rule or classifier. At the end of the first round, when all pixels have been allocated, the basic patterns can be altered in character according to the nature of the pixels that have been associated with them. If necessary, some basic patterns can be dropped from the analysis if only a small number of pixels are allocated to them, or, pairs of similar basic patterns can be combined by averaging. Also individual basic patterns can be split into two if they are thought to be too heterogeneous. The process of pixel labeling by association with one of the basic patterns is repeated using the updated basic patterns until the procedure converges, when the user will attempt to relate the basic patterns in the final cycle to some Earth surface cover class. It is important to realize that these two methods differ in that the supervised methods attempt to relate pixel groups with actual Earth-surface cover types; the pixel groups are thus termed information classes. The unsupervised methods simply determine the characteristics of non-overlapping groups of pixels in terms of their spectral band values. These groups are therefore known as spectral classes, and their relationship with information classes must be worked out through fieldwork and/or map and air

TABLE I. ISODATA Unsupervised Classification Procedure

1. Pick k_0 arbitrary centroids (mean vectors)
2. Classify the pixel vectors by assigning them to the class of the closest mean
3. *Standard deviation for each feature axis is comuted for each of the* k_0 *clusters*
   If a standard deviation > a prespecified thresshold, cluster is split along that axis
4. The distance between cluster centers is found
   If the distance is < a prespecified threshold, the two clusters are merged into one
5. *The process is repeated with the new* k_1 *number of clusters until no clusters are split or merged*

photograph interpretation. It is reasonable to assume that the impact of lossy compression will be nearly the same for the supervised and unsupervised classification of small-footprint imagery. For this reason, the supervised classification of small-footprint imagery is not considered in this article.

Unsupervised Classification

Unlike the supervised classification techniques, the unsupervised classification methods do not require the number of categories (species) and their statistical characteristics to be specified by the user in advance.

When there are insufficient statistical characteristics for the nature of the area covered, it would not be possible to estimate the mean centers of the classes (centroids). Even the number of such classes might not be known. In such cases we can only assume some initializations as a start then leave the classification procedure on its own to come up with suitable results. The relationship between the labels allocated by the classification criteria (classifier) to the pixels making up the multispectral image and the covered area types are determined after unsupervised classification has been carried out. Identification of the spectral classes picked out by the classifier in terms of "information classes" existing on the ground is achieved using whatever information is available to the analyst. The basic assumption on which these schemes are based is that the classes present in the data are compact, i.e., points associated with each class are tightly grouped around the class center, thus occupy a spherical region of feature space. A measure of the compactness of a class can be taken as the set of standard deviations for the class measured separately for each axis of feature space. If any of these standard deviations for a particular class is large, then that class is split in the direction of the axis concerned. A second assumption is that the classes are well separated, i.e., their centers are separated by a distance greater than a pre-selected threshold. Unsupervised classification is carried out via the general ISOADATA Procedure outlined in the Table I.

The Confusion Matrix

To evaluate the classification accuracy, the analyst selects a sample of pixels and then visits the sites (or vice-versa), then builds a confusion matrix. This is used to determine the nature and frequency of errors (nature of the errors: what kinds of information are confused; frequency of the errors: how often do they occur). The confusion matrix compares the relation between known reference data (ground truth) and the result of the automatic classification, so it tells how well the training samples of each class have been classified. The confusion matrix columns represent ground data (assumed to be correct), and the rows represent map data (classified by the automatic procedure). The diagonal elements represent agreement between ground and map, so ideally the matrix should be characterized by all zero off-diagonals.

The *errors of omission* (map producer's accuracy) are quantified as the number incorrect in a column divided by the total number in the column, hence measures how well the map maker was able to represent the ground features, i.e., it indicates how well the training set pixels of a given cover type are classified.

$$\text{Producer's Accuracy} = \frac{\text{Number of correctly classified pixels per category}}{\text{Number of reference pixels used for that category}} = \frac{\text{Diagonal element}}{\text{corresponding column total}}$$

The *errors of commission* (map user's accuracy) are the number incorrect in a row divided by the total number in that row, hence a measure how likely the map user is to encounter correct information while using the map, i.e., indicates the probability that a pixel classified into a category actually represents that category.

$$\text{User's Accuracy} = \frac{\text{Number of correctly classified pixels per category}}{\text{Number of pixels classified in that category}} = \frac{\text{Diagonal element}}{\text{corresponding row total}}$$

The map *overall accuracy* is the total on diagonal divided by the grand total.

Classification of Large-Footprint Spectral Imagery Data

For large-footprint imagery, such as those from NOAA's AVHRR sensor with a 1.1 km footprint, accurate land cover estimation can only be achieved if each pixel is assigned not just to one, but several labels along with their respective concentrations in that pixel's footprint. The technique used to assign these labels and proportions is known as mixture modeling, or spectral unmixing. Spectral unmixing produces a compositional map, also known as abundance image, that provides a more complete land cover type information than a thematic map. The set of compositional maps depicts the proportions of all species present in each pixel footprint, while the thematic map identifies only the species with the highest concentration. Thus, it can be argued that spectral unmixing yields a more complete classification information than a thematic map. Since the number and the signitures of species in the scene is provided in advance, the process of spectral unmixing can be considered as a "supervised" form of classification for large-footprint imagery.

Linear Spectral Pixel Unmixing

Linear pixel unmixing, also known as linear mixture modeling, assumes that the spectral signature of each pixel vector is the linear combination of a limited set of fundamental spectral components known as end members. Assume that each species within a pixel footprint contributes to the signal received at the satellite sensor an amount characteristic of that species and proportional to the area covered by it. The conventional spectral unmixing is modeled as,

$$\mathbf{x} = \mathrm{M}\,\mathbf{f} + \mathbf{e} \quad (1)$$
$$= f_1\,\mathbf{m}_1 + f_2\,\mathbf{m}_2 + \ldots + f_i\,\mathbf{m}_i + \ldots + f_n\,\mathbf{m}_{Nm} + \mathbf{e}$$

where:

$\mathbf{x}$	a pixel signature of N_b components
M	$N_b \times N_m$ matrix of end members $\mathbf{m}_{1,\ldots \mathrm{Nm}}$
f_i	fractional component of end member i , i.e., proportion of footprint covered by species i
$\mathbf{f}$	vector of fractional components $(f_1, f_2, \ldots f_i, \ldots f_{Nm})^{\mathrm{tr}}$
$\mathbf{m}_i$	end member i of N_b components
e	residual error vector of N_b components
N_m	number of end members
N_b	number of spectral bands
N_c	Intrinsic true spectral dimension of data, $N_c \le N_b$

Provided that the number of end members $N_m \le N_c$, the solution via classical least squares estimation is,

$$f = (M^T M)^{-1} M^T x \quad (2)$$

Selection of the Optimum Subset of End members

When the number of end members is more than the true spectral dimensionality of the scene, i.e., $N_m > N_c$, we encounter the so-called Condition of identifiability , which means that f can not be determined via Eq. (2). This situation may seriously restrict the applicability of the linear umixing operation since most operational remote sensing systems measure radiation in limited number of bands. Therefore, the scene can be decomposed into only a limited number of distinct components. For example for Landsat TM with seven spectral bands (Nb = 7), the true spectral dimension is at most five (Nc = 5) based on principal component analysis. To overcome the condition of identifiability, we adopted the method of dynamic selection of optimum end member subset recently proposed by Maselli.[5] In this technique, an optimum subset of all available end members is selected for spectral unmixing of each pixel vector in the scene. Thus, although not every pixel vector will have a fractional component for each end members, the ensemble of all pixel vectors in the scene will collectively have fractional contributions for each end member.

For each pixel vector, a unique subset of the available end members is selected which minimizes the residual error after decomposition of that pixel vector. To determine the $\mathrm{N_c}$ optimum end members for pixel vector x, the pixel vector is projected onto all available normalized end members.[6] The most efficient projection, which corresponds to the highest dot product value $c_{\max}$, indicates the first selected end member $\mathbf{m}_{\max}$. It can be shown that this procedure is equivalent to finding the end member with the smallest spectral angle with respect to $\mathbf{x}$. The residual pixel signature, $\mathrm{r}_{\mathbf{x}} = \mathbf{x} - c_{\max} \cdot \mathbf{m}_{\max}$ is then used to identify the second end member by repeating the projection onto all remaining end members. The process continues up to the identification of a prefixed maximum N_c number of end members from the total of N_e available end members.

Displaying the Species Concentration Maps

The proposed spectral unmixing procedure produces the species concentrations as fractional, floating point, values. For display and storage purposes, these floating point maps should be converted into integer format. This requires a quantization process. For compression and archival applications, it is desirable to minimize the quantization error induced by the quantizer. For this purpose the following nonlinear mapping scheme was adopted.

$$M = \frac{255 f^{\exp}}{f_{\max}|f_{\max}|^{(\exp-1)} - f_{\min}|f_{\min}|^{(\exp-1)}} + 0.5 \quad (3)$$

where:

M	=	mapped integer fractional component in the range of $0 \le M \le 255$
f	=	fractional component
$f_{\min}$	=	minimum fractional component
$f_{\max}$	=	maximum fractional component
exp	=	floating point exponent parameter in the range of $0 \le \exp \le 1.0$

Note that for exp = 1 Eq. (3) reduces to simple linear mapping. The optimum value of exp was determined, empirically, to be 0.6 for the test abundance images. The RMS quantization error for the optimum nonlinear mapping was about 30% lower than that for the linear mapping.

Criteria to Measure Compression Impact on Classification

To assess the impact of compression on classification, we have adopted the following two machine-based quantitative measures. For either of the two assessment schemes, the compression rate is varied across a predefined range.

For classification of small-footprint imagery the impact of compression is assessed via comparing the resulting thematic map. Comparison is achieved via obtaining a confusion matrix from the thematic maps corresponding to the original and reconstructed spectral images.

For large-footprint imagery the impact of compression is assessed via comparing the two sets of abundance images obtained from the original and reconstructed image sets. Comparison can be performed via obtaining some statistical measures such as mean square, maximum, and standard deviation of, errors for each corresponding pair of abundance images. In the experiment reported here, the comparison has been performed with respect to the resulting mean absolute error.

Experimental Results

The compression, classification, and spectral unmixing were implemented in C programming language and applied to different sets of multispectral imagery from different sensor platforms. The programs were conveniently parameterized to accommodate various system parameters including the compression ratio, dynamic range of data, number of spectral bands, image sizes, convergence threshold, and number of classes.

Two sets of imagery data, one with small footprint and one with large footprint, were selected for our experiments. The small footprint (30 m) imagery set consisted on seven 512 × 512, 8 bits per pixel LANDSAT TM spectral images of a scene in Montana. The large footprint (1.1 km) imagery set consisted of five 1024 × 1024, 10 bits per pixel NOAA's AVHRR spectral images of UK. These two test sets are shown in Figs. 2 and 3 respectively.

Figure 4 shows the resulting color thematic maps for the original Montana test set and its compressed/reconstructed versions at a compression ratio of 8, which corresponds to a coding bit rate of 1 bits per pixel. A total of 14 classes are chosen for the classification procedure. Visual inspection of the thematic maps does not reveal many changes in the outlined classes. To accurately register the changes we resorted to confusion

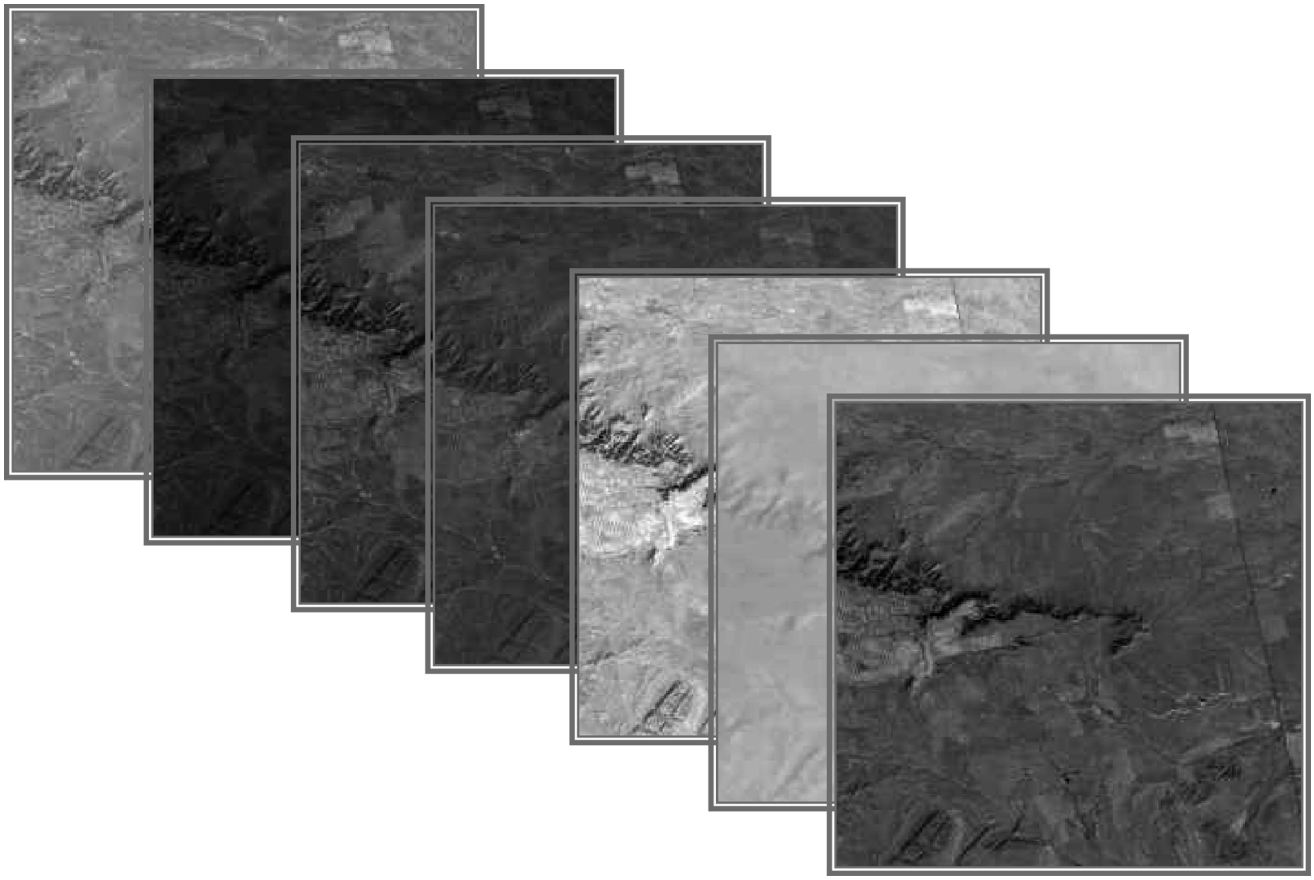

Figure 2. Small footprint test set (seven 512 × 512, 8 bits per pixel LANDSAT TM spectral images of a scene in Montana, footprint = 30 m)

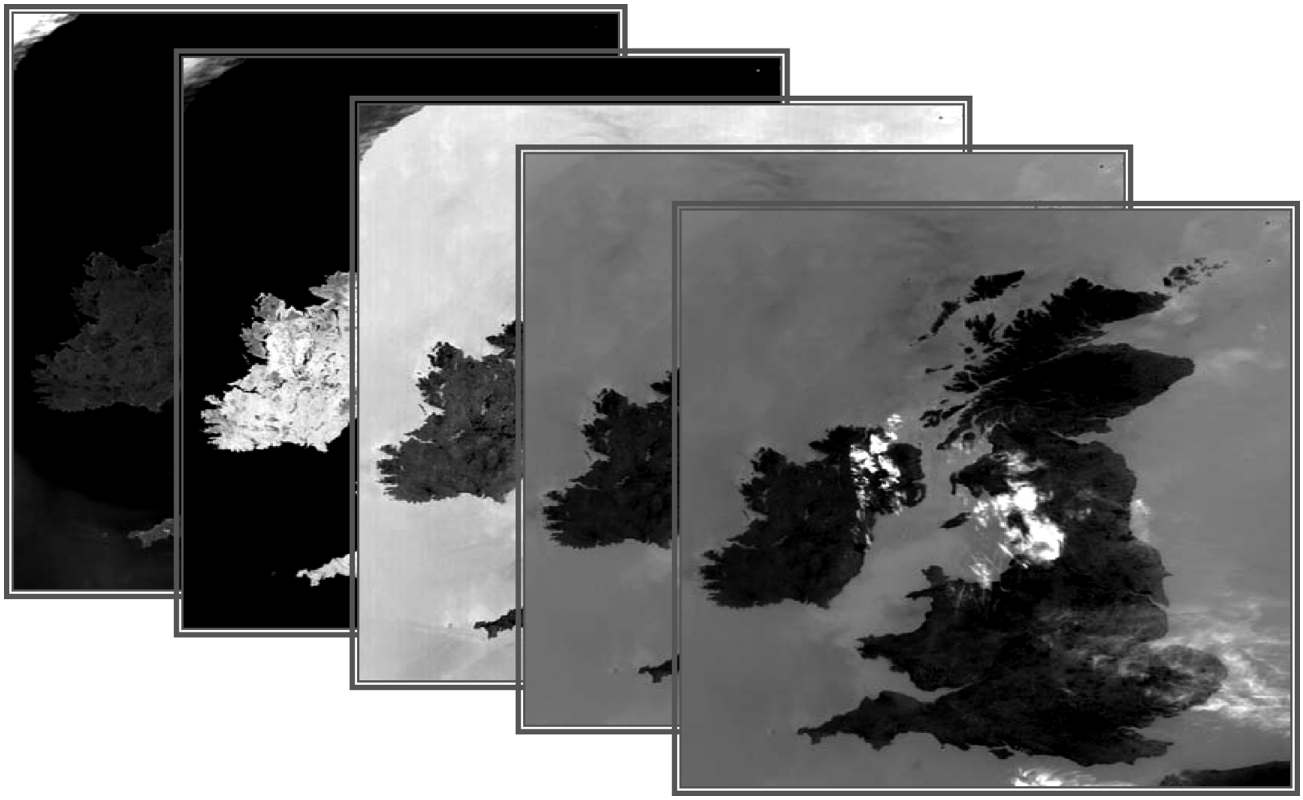

Figure 3. Large footprint test set (five 1024 × 1024, 10 bits per pixel NOAA's AVHRR spectral images of UK, footprint = 1.1 km)

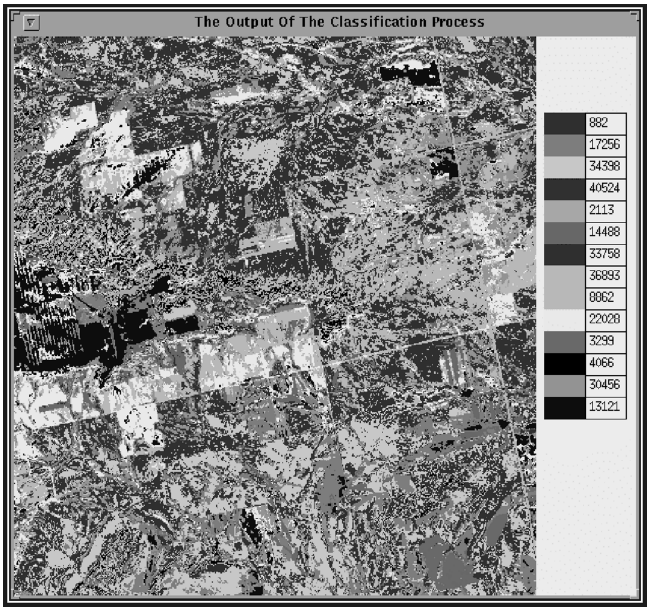

(a)

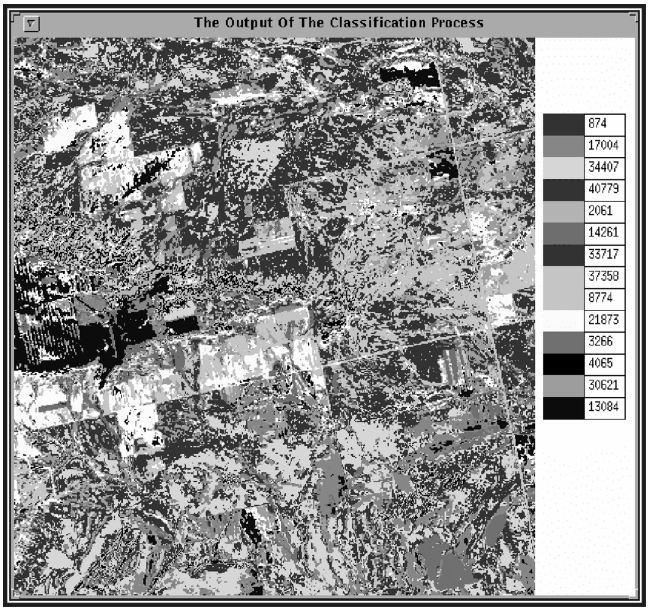

(b)

Figure 4. 14-class thematic map produced from (a) the original Montana test set and (b) its reconstruction at 8-to-1 compression ratio

Class No.	0	1	2	3	4	5	6	7	8	9	10	11	12	13	Row Sum	Producer Accuracy
0	**817**	**0**	**0**	**0**	**1**	**0**	**0**	**0**	**1**	**48**	**0**	**1**	**0**	**6**	**874**	0.935
1	**0**	**13937**	**940**	**906**	**0**	**237**	**0**	**0**	**0**	**0**	**42**	**0**	**754**	**188**	**17004**	0.820
2	**0**	**1043**	**28572**	**2880**	**0**	**415**	**1446**	**1**	**3**	**0**	**47**	**0**	**0**	**0**	**34407**	0.830
3	**0**	**896**	**2709**	**31201**	**0**	**765**	**1769**	**1445**	**0**	**2**	**0**	**0**	**1992**	**0**	**40779**	0.765
4	**0**	**0**	**0**	**0**	**1871**	**0**	**0**	**0**	**0**	**0**	**0**	**190**	**0**	**0**	**2061**	0.908
5	**0**	**246**	**410**	**723**	**0**	**10497**	**682**	**724**	**182**	**112**	**178**	**0**	**502**	**5**	**14261**	0.736
6	**0**	**0**	**1637**	**1844**	**0**	**705**	**27105**	**1556**	**862**	**0**	**7**	**0**	**1**	**0**	**33717**	0.804
7	**1**	**0**	**0**	**1496**	**0**	**838**	**1621**	**30506**	**345**	**910**	**0**	**0**	**1641**	**0**	**37358**	0.817
8	**0**	**0**	**1**	**0**	**0**	**142**	**964**	**256**	**7002**	**0**	**10**	**399**	**0**	**0**	**8774**	0.798
9	**60**	**0**	**0**	**1**	**0**	**114**	**0**	**873**	**0**	**18700**	**1**	**0**	**1528**	**596**	**21873**	0.855
10	**0**	**37**	**49**	**0**	**0**	**163**	**5**	**0**	**12**	**0**	**2992**	**1**	**0**	**7**	**3266**	0.916
11	**0**	**0**	**0**	**0**	**230**	**0**	**0**	**0**	**359**	**0**	**1**	**3475**	**0**	**0**	**4065**	0.855
12	**0**	**725**	**0**	**1937**	**0**	**538**	**0**	**1604**	**0**	**1734**	**0**	**0**	**23702**	**381**	**30621**	0.774
13	**14**	**171**	**0**	**0**	**0**	**1**	**0**	**0**	**0**	**594**	**6**	**0**	**340**	**11958**	**13084**	0.914
Column Sum	**892**	**17055**	**34318**	**40988**	**2102**	**14415**	**33592**	**36965**	**8766**	**22100**	**3284**	**4066**	**30460**	**13141**	**262144**	
User Accuracy	0.916	0.817	0.833	0.761	0.890	0.728	0.807	0.825	0.799	0.846	0.911	0.855	0.778	0.910		0.810

Figure 5. Confusion matrix for Montana thematic map at compression ratio of 8

matrix evaluation. Figure 5 shows the corresponding confusion matrix. Figure 6 depicts the overall accuracy versus the compression ratio. It can be observed from the graphs that, at an 8-to-1 compression ratio, more than 81 percent of the pixels will be classified the same as done with the original imagery data. This, however, should not be interpreted as a loss of 19 percent in classification accuracy due to an 8-to-1 compression. The impact is much smaller since the pixel classification based on the original data is not perfect either. Even without compression, it is common to misclassify more than 10 percent of the pixels due to others sources of inaccuracies in the original data and the relevant prediction models. For this reason it is reasonable to assume that the impact of compression on classification is insignificant at compression ratios on less than 8.

Figure 7 shows the results of spectral unmixing applied to the original data and its reconstruction at 10-to-1 compression ratio, i.e., one bit per pixel coding bit rate. Visual examination does not reveal any changes between the resulting two sets of abundance images. Figure 8 shows the corresponding difference images that are contrast-stretched to reveal any residual structures present. The mean absolute difference between each pair

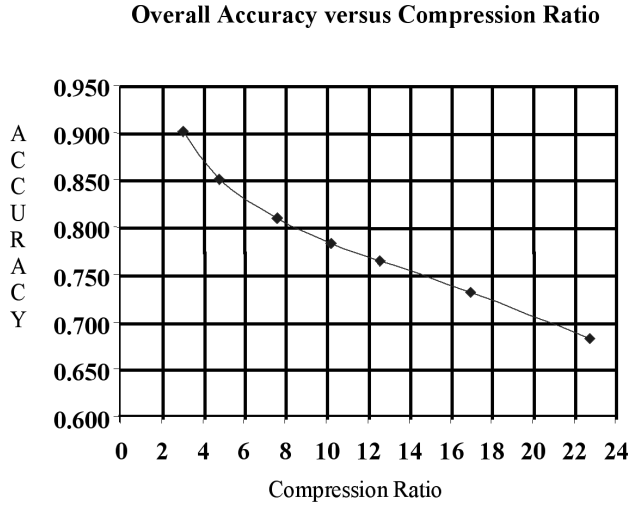

Figure 6. The Overall Accuracy with different Compression Ratios

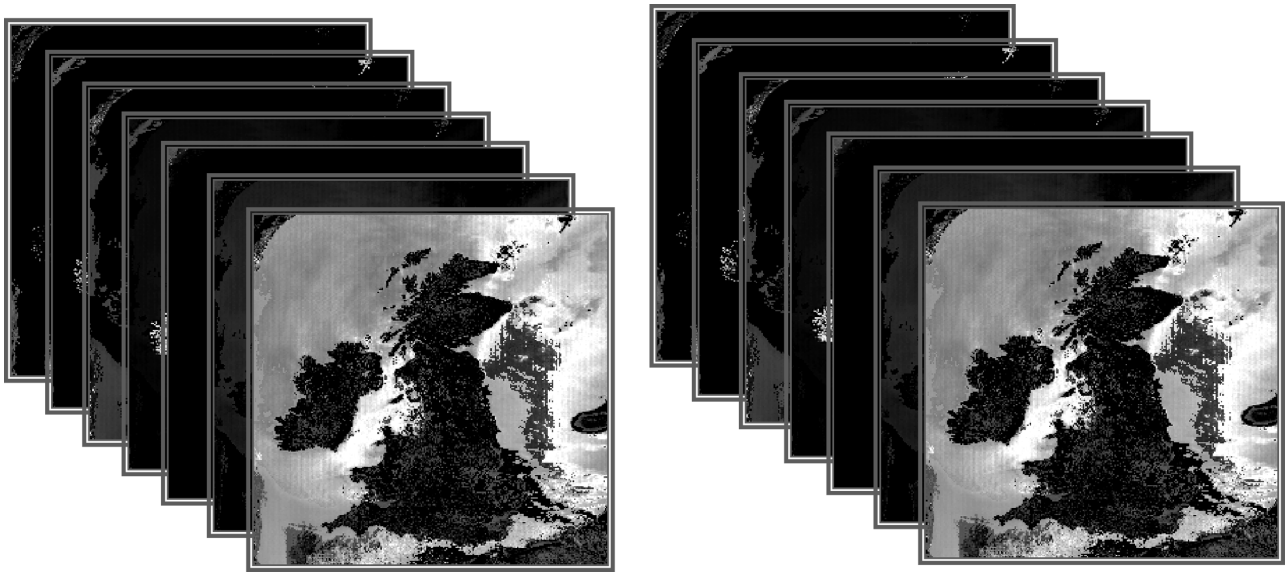

(a) (b)

Figure 7. Spectral unmixing results for (a) the original data, and (b) reconstructed data at a compression ratio of 10-to-1.

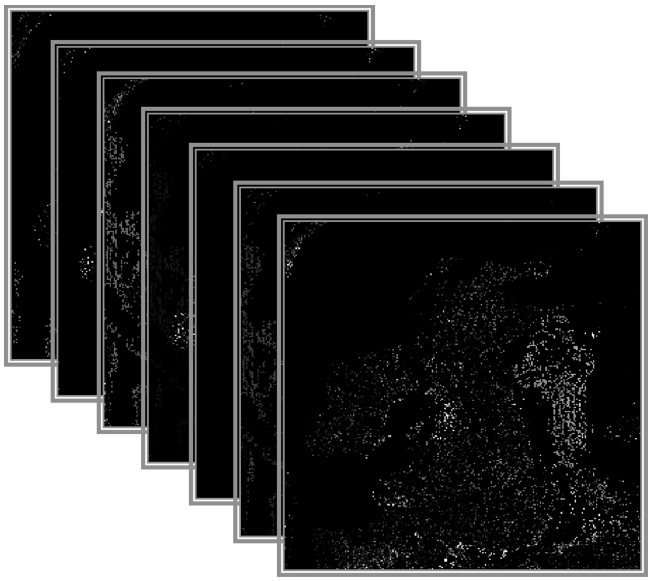

Figure 8. The difference images between abundance image sets in Fig. 7

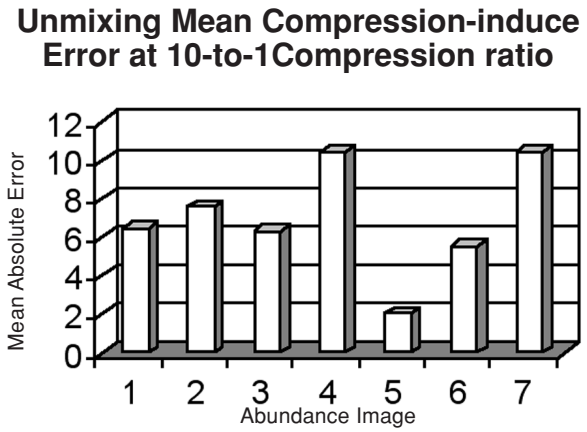

Figure 9. Mean absolute differences between pairs of corresponding abundance image in Fig. 8.

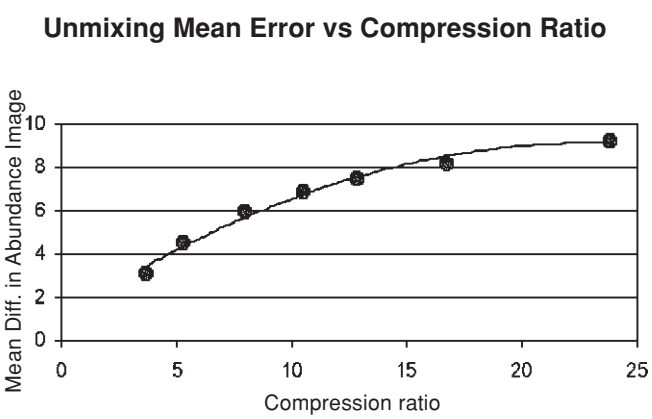

Figure 10. Mean absolute difference versus compression ratio between abundance images obtained from the original and reconstructed data sets

of abundance images appears in Fig. 9. The impact of compression ratio on the average mean abundance image difference is shown in Fig. 10 for various compression ratios. It can be observed that at an 8-to-1 compression ratio, the resulting mean absolute difference is about six percent. Again, considering the presence of other sources of inaccuracies in the original data and the relevant prediction models, the effective loss of fidelity of the pixels in the abundance images (at 8-to-1 compression ratio) is likely in the order of three percent. Thus a compression ratio of 8-to-1 is likely to have insignificant impact on classification of large-footprint AVHRR imagery as well.

Conclusion

The impact of lossy compression on the classification of the remotely–sensed imagery data was examined. The impact of compression was assessed for both types of classifications, i.e., classification via thematic map for small-footprint imagery, and classification via spectral unmixing (decomposition into abundance images) for large-footprint imagery. Experimental results. It was shown the impact of compression is insignificant for compression ratios of less than 8.

In general, the quality of the final product derived from the data is based on the interaction of several processing components, which include the precision of the original data as well as the accuracy of the relevant prediction models. Lossy compression of sensor data can also be considered as an additional component in the accuracy of the final product. As such, the effective impact of compression is reduced by the presence of these others sources of inaccuracies in the data. ⚠

Acknowledgment. The work reported in this article was supported in part by US Department of Navy, Office of Naval Research, award number N00014-01-1-1049, technical representative George W. Solhan.

References

1. C. Lambert-Nebout, G. Gmoury and J. E. Blamont, Status of Onboard Compression for CNES Space Missions, *Proc. SPIE* **3808,** pp. 242–255 (1999).
2. J. A. Saghri, A. G. Tescher and J. T. Reagan, Spaced-based Data Compression Issues, *J. Electronic Imaging* **8**(3), 301–310 (1999).
3. J. A. Saghri, A. G. Tescher and J. T. Reagan, Practical Transform Coding of Multispectral Imagery, *IEEE Signal Processing Magazine* **12**(1), 32–43 (1995).
4. J. A. Saghri, A. G. Tescher and A. Boujarwah, Spectral-signature preserving Compression of Multispectral Data, *Optical Engineering* **38**(12), 2081–2088 (1999).
5. F. Maselli, Multiclass Spectral Decomposition of Remotely Sensed Scenes by Selective Pixel Unmixing, *IEEE Trans. Geoscience and Remote Sensing* **36**(5), 1809–1819 (1998).
6. J. A. Saghri, A. G. Tescher, F. Jaradi, and M. Omran, A Viable End-Member Selection Scheme for Spectral Unmixing of Multispectral Satellite Imagery Data, *J. Imaging Sci. Technol.* **44**(3), 196–203 (2000).